Inorg. Chem. **2005**, *44*, 1571–1579

Unusual Monodentate Binding Mode of 2,2′-Dipyridylamine (L) in Isomeric *trans*-$(acac)_2Ru^{II}(L)_2$, *trans*-$[(acac)_2Ru^{III}(L)_2]ClO_4$, and *cis*-$(acac)_2Ru^{II}(L)_2$ (acac = Acetylacetonate). Synthesis, Structures, and Spectroscopic, Electrochemical, and Magnetic Aspects

Sanjib Kar,[†] Nripen Chanda,[†] Shaikh M. Mobin,[†] Francisco A. Urbanos,[‡] Mark Niemeyer,[§] Vedavati G. Puranik,[||] Reyes Jimenez-Aparicio,*[,‡] and Goutam Kumar Lahiri*[,†]

Department of Chemistry, Indian Institute of Technology−Bombay, Powai, Mumbai-400076, India, Departamento de Química Inorgánica, Facultad de Ciencias Químicas, Universidad Complutense, Ciudad Universitaria, E28040-Madrid, Spain, Institut für Anorganische Chemie, Universität Stuttgart, Pfaffenwaldring 55, D-70569 Stuttgart, Germany, and Center for Materials Characterization, National Chemical Laboratory, Pune, Maharashtra-411008, India

Received June 16, 2004

The reaction of *cis*-$Ru(acac)_2(CH_3CN)_2$ (acac = acetylacetonate) with 2,2′-dipyridylamine (L) in ethanolic medium resulted in facile one-pot synthesis of stable $[(acac)_2Ru^{III}(L)]ClO_4$ ([**1**]ClO_4), *trans*-$[(acac)_2Ru^{II}(L)_2]$ (**2**), *trans*-$[(acac)_2Ru^{III}(L)_2]ClO_4$ ([**2**]ClO_4), and *cis*-$[(acac)_2Ru^{II}(L)_2]$ (**3**). The bivalent congener **1** was generated via electrochemical reduction of [**1**]ClO_4. Although in $[\mathbf{1}]^+$ the dipyridylamine ligand (L) is bonded to the metal ion in usual bidentate fashion, in **2**/$[\mathbf{2}]^+$ and **3**, the unusual monodentate binding mode of L has been preferentially stabilized. Moreover, in **2**/$[\mathbf{2}]^+$ and **3**, two such monodentate L's have been oriented in the *trans*- and *cis*-configurations, respectively. The binding mode of L and the isomeric geometries of the complexes were established by their single-crystal X-ray structures. The redox stability of the Ru(II) state follows the order **1** < **2** ≪ **3**. In contrast to the magnetic moment obtained for [**1**]ClO_4, $\mu = 1.84\ \mu_B$ at 298 K, typical for low-spin Ru(III) species, the compound [**2**]ClO_4 exhibited an anomalous magnetic moment of 2.71 μ_B at 300 K in the solid state. The variable-temperature magnetic measurements showed a pronounced decrease of the magnetic moment with the temperature, and that dropped to 1.59 μ_B at 3 K. The experimental data can be fitted satisfactorily using eq 2 that considered nonquenched spin–orbit coupling and Weiss constant in addition to the temperature-independent paramagnetism. [**1**]ClO_4 and [**2**]ClO_4 displayed rhombic and axial EPR spectra, respectively, in both the solid and the solution states at 77 K.

Introduction

2,2′-Dipyridylamine (L) has been widely used in synthesizing a large number of mononuclear[1] and polynuclear[2] metal complexes with varying perspectives. At the mononuclear level, in almost all occasions it has been found to behave expectedly as a bidentate chelating ligand, mostly bonded through its two terminal pyridine nitrogen donors (**A**). However, in certain mononuclear aluminum complexes, the chelate ring is also known to form selectively via one of the terminal pyridine nitrogens and the central anionic amido nitrogen (**B**).[3] The monodentate binding mode of L (**C**) has been confined to only a limited number of complexes, metal−metal bonded $[Ru(CH_3CO_2)(CO)_2(L)]_2$,[4a] linear $[(PPh_3)Au(L)]ClO_4$,[4b] octahedral $M(CO)_3(bpy)(L)$ [M = Mo,W; bpy = 2,2′-bipyridine],[4c] $W(CO)_5(L)$,[4d] and polymeric $[(L)_2Pb(OAc)_2]$.[4e]

In those occasions, the available sixth coordination site in the cases of octahedral Ru, Mo, and W and the second coordination site in the linear Au-complex were essentially satisfied by the monodentate form of L. The preferential stabilization of the unusual monodentate motif (**C**) of L instead of the usual bidentate motif (**A**) was primarily directed by the selective availability of only one coordination site around

* Author to whom correspondence should be addressed. E-mail: lahiri@chem.iitb.ac.in.
[†] Indian Institute of Technology−Bombay.
[‡] Universidad Complutense.
[§] Universität Stuttgart.
[||] National Chemical Laboratory.

10.1021/ic049219v CCC: $30.25
Published on Web 02/08/2005

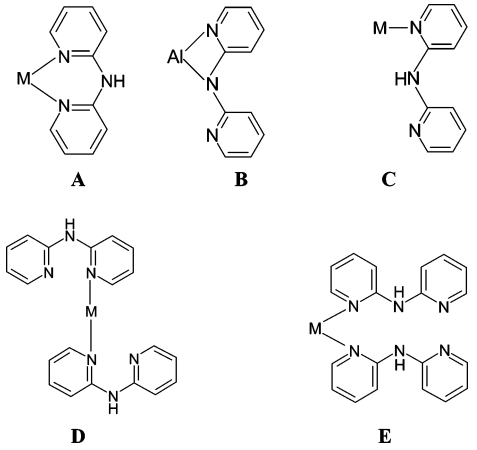

the metal ion. In $(L)_2Pb(OAc)_2$, the *trans*-disposition of symmetry-related monodentate L around Pb led to a linear polymer via the oxygen atom of the acetate unit.

The present article demonstrates a unique metal−ligand combination of $\{Ru(acac)_2\}$ (acac = acetylacetonate) and L which facilitates the stabilization of the rather rare monodentate binding mode of L, simultaneously in both the *trans*-$Ru(acac)_2(L)_2$ (motif **D**) and the *cis*-$Ru(acac)_2(L)_2$ (motif **E**) configurations along with the most likely bidentate mode of L in $Ru(acac)_2(L)$ (motif **A**).

In this paper, we report the facile one-pot synthesis of $[(acac)_2Ru^{III}(L)]ClO_4$ ([**1**]ClO_4), *trans*-$[(acac)_2Ru^{II}(L)_2]$ (**2**), *trans*-$[(acac)_2Ru^{III}(L)_2]ClO_4$ ([**2**]ClO_4), and *cis*-$[(acac)_2Ru^{II}(L)_2]$ (**3**). The crystal structures of all four members, [**1**]ClO_4, **2**, [**2**]ClO_4, and **3**, and their spectroscopic, electrochemical, and magnetic aspects have been scrutinized.

Results and Discussion

The reaction of 2,2′-dipyridylamine (L) with the metal precursor, *cis*-$Ru^{II}(acac)_2(CH_3CN)_2$ (acac = acetylacetonate), in a 2:1 molar ratio in ethanol under air followed by chromatographic operation of the initial product using a silica gel column resulted in one-pot synthesis of four complexes, diamagnetic *trans*-$[(acac)_2Ru^{II}(L)_2]$ (**2**), and *cis*-$[(acac)_2Ru^{II}(L)_2]$ (**3**), as well as paramagnetic $[(acac)_2Ru^{III}(L)]ClO_4$ ([**1**]ClO_4) and *trans*-$[(acac)_2Ru^{III}(L)_2]ClO_4$ ([**2**]ClO_4) (Scheme 1) in a ratio of approximately 1:1: 2.25:1.5. However, the use of a lower amount of L, that is, L:metal precursor, 1:1, led to the increase in the yield of the expected chelated product ([**1**]ClO_4) with the concomitant decrease in yield of the complexes incorporating monodentate L, **2**, [**2**]ClO_4, and **3** (approximate ratio of the products, **2**:**3**:[**1**]ClO_4:[**2**]ClO_4 = 1:1:6.5:1). Further, the use of a higher L:M ratio (3:1) did not make any significant change in the relative yields of the products as compared to the initial 2:1 ratio. Therefore, the 2:1 ratio of L and M was followed.

The bivalent congener $[(acac)_2Ru^{II}(L)]$ (**1**) can be easily generated via the electrochemical reduction of $[\mathbf{1}]^+$, but it was found to be susceptible to undergo facile oxidation to trivalent $[\mathbf{1}]^+$ under atmospheric conditions, in keeping with its low ruthenium(III/II) reduction potential, −0.29 V versus SCE (see later). However, the bivalent complex **2** is reasonably stable even in atmospheric conditions and only slowly oxidizes to the corresponding trivalent $[\mathbf{2}]^+$ despite its sufficiently low ruthenium(III)−ruthenium(II) potential, −0.15 V versus SCE. On the other hand, the trivalent $[\mathbf{3}]^+$ was found to be unstable even on the coulometric time scale (see later).

Scheme 1 [a]

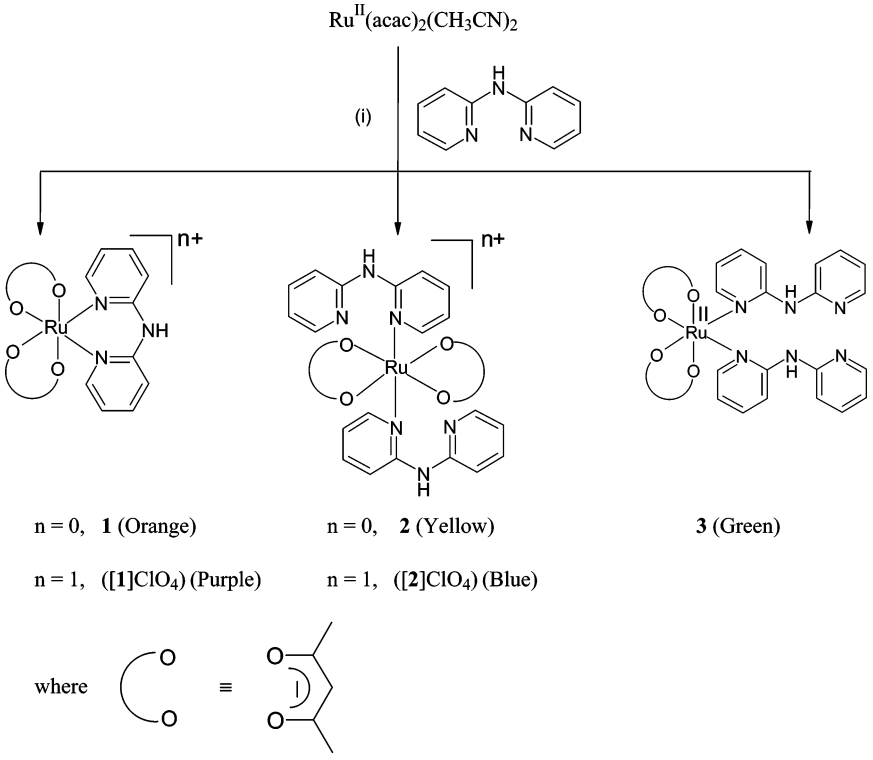

[a] (i) EtOH, Δ, stir.

Although in $[\mathbf{1}]^+$ the dipyridylamine ligand (L) is bonded to the metal ion in usual bidentate fashion, in **2**/$[\mathbf{2}]^+$ and **3**, the unusual monodentate binding mode of L has been preferentially stabilized. Moreover, in **2**/$[\mathbf{2}]^+$ and **3**, two such monodentate L's have been oriented in the *trans*- and *cis*-configurations, respectively. The *cis*-orientation of two such bulkier monodentate L's in **3** appears to be most surprising particularly where the usual *cis*-bidentate mode of L (motif **A**) is also found to be simultaneously equally stable in $[\mathbf{1}]^+$ or **1**. All four complexes {$[\mathbf{1}]^+$, **2**/$[\mathbf{2}]^+$, and **3**} are stable with respect to isomerization in both the solid and the solution states. The conversion of **3** to **1** or $[\mathbf{1}]^+$ did not take place even in boiling CH_3CN or C_2H_5OH. Similarly, no conversion of **1** or $[\mathbf{1}]^+ \rightarrow$ **3** was observed in the presence of excess L in boiling acetonitrile. The feasibility of the conversion of **3** $\rightarrow$ **2**/$[\mathbf{2}]^+$ or vice versa was also checked under heating condition in acetonitrile medium, but they had shown total inertness toward any sort of transformations. This implies that L preferentially binds either in monodentate or in bidentate fashion independently during the course of the reaction based on the L:M ratio, 2:1 or 1:1.

The chelated form of L in **1** or $[\mathbf{1}]^+$ is expected to be thermodynamically more stable than its monodentate form either in *cis* (**3**)- or in *trans* (**2**)-isomer. However, the fact that neither **3** nor **2** can be converted into the chelated form **1** or $[\mathbf{1}]^+$ even by subjecting to a temperature of ~80 °C (boiling CH_3CN or C_2H_5OH) probably indicates that the kinetic barriers, for such conversions, are sufficiently high.

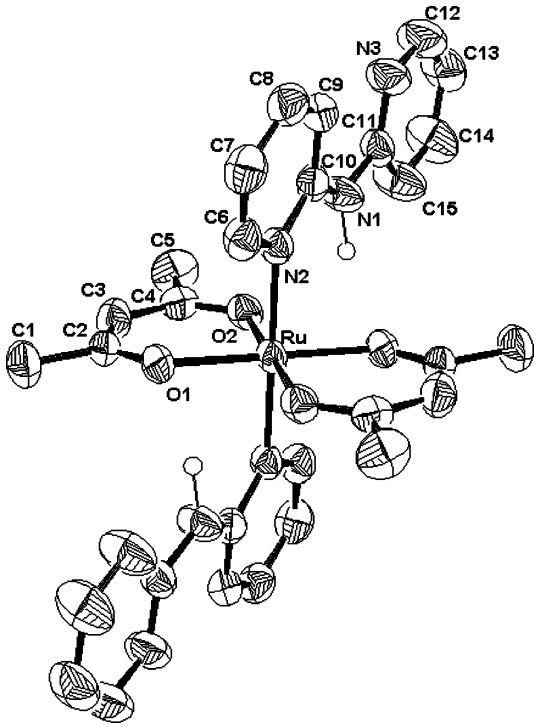

Figure 1. ORTEP diagram of **2**. Hydrogen atoms, with the exception of the N-bonded one, have been omitted for clarity. Ellipsoids are drawn at 50% probability.

In other words, the stability of **3** and **2** isomers is primarily kinetic rather than thermodynamic in origin.

Simple substitution of the solvent molecules (CH_3CN) by L in *cis*-$Ru^{II}(acac)_2(CH_3CN)_2$ is expected to yield either chelated (**1**) or the monodentate *cis*-isomer (**3**). Dissociation of one CH_3CN from the precursor complex would lead to a five-coordinate intermediate, which by Berry pseudorotation could equilibrate to a trigonal bipyramidal (tbp) and a square pyramidal (sp) geometry. The latter, on addition of a second L, will yield the *trans*-isomer (**2**) (Scheme S1, Supporting Information).[5]

The complexes exhibited satisfactory microanalytical data. $[\mathbf{1}]ClO_4$ and $[\mathbf{2}]ClO_4$ showed 1:1 conductivity in acetonitrile. The formation of the complexes was evidenced by their electrospray mass spectral data in acetonitrile (see the Experimental Section).

The binding modes of L in the complexes were authenticated by their single-crystal X-ray structures (Figures 1 and 2, Figures S1 and S2, and Tables 1 and 2). In $[\mathbf{1}]ClO_4$, the dipyridylamine (L) is bonded in its usual bidentate mode, whereas in **2**/$[\mathbf{2}]ClO_4$ and **3** two monodentate L's [bonded through one of the pyridine nitrogen donor centers N(2)] are

(1) Selective references: (a) Haukka, M.; Da Costa, P.; Luukkanen, S. *Organometallics* **2003**, *22*, 5137. (b) Gerber, T. I. A.; Abrahams, A.; Mayer, P.; Hosten, E. *J. Coord. Chem.* **2003**, *56*, 1397. (c) Rauterkus, M. J.; Fakih, S.; Mock, C.; Puscasu, I.; Krebs, B. *Inorg. Chim. Acta* **2003**, *350*, 355. (d) Moreno, Y.; Vega, A.; Ushak, S.; Baggio, R.; Pena, O.; Le Fur, E.; Pivan, J.-Y.; Spodine, E. *J. Mater. Chem.* **2003**, *13*, 2381. (e) Tsujimura, S.; Kano, K.; Ikeda, T. *Chem. Lett.* **2002**, *10*, 1022. (f) Youngme, S.; Chaichit, N.; Koonsaeng, N. *Inorg. Chim. Acta*. **2002**, *335*, 36. (g) Madureira, J.; Santos, T. M.; Goodfellow, B. J.; Lucena, M.; Pedrosa de Jesus, J.; Santana-Marques, M. G.; Drew, M. G. B.; Félix, V. *J. Chem. Soc., Dalton Trans.* **2000**, 4422. (h) Santos, T. M.; Goodfellow, B. J.; Madureira, J.; Pedrosa de Jesus, J.; Félix, V.; Drew, M. G. B. *New J. Chem.* **1999**, 1015. (i) Anderson, P. A.; Deacon, G. B.; Haarmann, K. H.; Keene, F. R.; Meyer, T. J.; Reitsma, D. A.; Skelton, B. W.; Strouse, G. F.; Thomas, N. C.; Treadway, J. A.; White, A. H. *Inorg. Chem.* **1995**, *34*, 6145. (j) Nagao, N.; Mukaida, M.; Tachiyashiki, S.; Mizumachi, K. *Bull. Chem. Soc. Jpn.* **1994**, *67*, 1802. (k) Kumagai, H.; Kitagawa, S.; Maekawa, M.; Kawata, S.; Kiso, H.; Munakata, M. *J. Chem. Soc., Dalton Trans*. **2002**, 2390. (l) Morris, D. E.; Ohsawa, Y.; Segers, D. P.; DeArmond, M. K.; Hanck, K. W. *Inorg. Chem.* **1984**, *23*, 3010. (m) Blakley, R. L.; DeArmond, M. K. *J. Am. Chem. Soc.* **1987**, *109*, 4895. (n) Blakley, R. L.; Myrick, M. L.; DeArmond, M. K. *J. Am. Chem. Soc.* **1986**, *108*, 7843. (o) Segers, D. P.; DeArmond, M. K. *J. Phys. Chem.* **1982**, *86*, 3768.

(2) Selective references: (a) Sheu, J. T.; Lin, C.-C.; Chao, I.; Wang, C.-C.; Peng, S.-M. *J. Chem. Soc., Chem. Commun.* **1996**, 315. (b) Berry, J. F.; Cotton, F. A.; Daniels, L. M.; Murillo, C. A.; Wang, X. *Inorg. Chem.* **2003**, *42*, 2418. (c) Berry, J. F.; Cotton, F. A.; Lei, P.; Lu, T.; Murillo, C. A. *Inorg. Chem.* **2003**, *42*, 3534. (d) Berry, J. F.; Cotton, F. A.; Lei, P.; Murillo, C. A. *Inorg. Chem.* **2003**, *42*, 377. (e) Berry, J. F.; Cotton, F. A.; Lu, T.; Murillo, C. A.; Wang, X. *Inorg. Chem.* **2003**, *42*, 3595. (f) Tsao, T.-B.; Lee, G.-H.; Yeh, C.-Y.; Peng, S.-M. *Dalton Trans.* **2003**, 1465. (g) Clerac, R.; Cotton, F. A.; Dunbar, K. R.; Lu, T.; Murillo, C. A.; Wang, X. *J. Am. Chem. Soc.* **2000**, *122*, 2272. (h) Rohmer, M.-M.; Strich, A.; Benard, M.; Malrieu, J.-P. *J. Am. Chem. Soc.* **2001**, *123*, 9126. (i) Berry, J. F.; Cotton, F. A.; Lu, T.; Murillo, C. A. *Inorg. Chem.* **2003**, *42*, 4425. (j) Cabeza, J. A.; del Río, I.; García-Granda, S.; Riera, V.; Suárez, M. *Organometallics* **2002**, *21*, 2540.

(3) (a) Engelhardt, L. M.; Gardiner, M. G.; Jones, C.; Junk, P. C.; Raston, C. L.; White, A. H. *J. Chem. Soc., Dalton Trans.* **1996**, 3053. (b) Ashenhurst, J.; Brancaleon, L.; Gao, S.; Liu, W.; Schmider, H.; Wang, S.; Wu, G.; Wu, Q. G. *Organometallics* **1998**, *17*, 5334.

(4) (a) Kepert, C. M.; Deacon, G. B.; Spiccia, L. *Inorg. Chim. Acta* **2003**, *355*, 213. (b) Munakata, M.; Yan, S.-G.; Maekawa, M.; Akiyama, M.; Kitagawa, S. *J. Chem. Soc., Dalton Trans.* **1997**, 4257. (c) Howie, R. A.; McQuillan, G. P. *J. Chem. Soc., Dalton Trans.* **1986**, 759. (d) Creaven, B. S.; Howie, R. A.; Long, C. *Acta Crystallogr*. **2000**, *C56*, e181. (e) Harrowfield, J. M.; Miyamae, H.; Skelton, B. W.; Soudi, A. A.; White, A. H. *Aust. J. Chem.* **1996**, *49*, 1121.

(5) Bennett, M. A.; Chung, G.; Hockless, D. C. R.; Neumann, H.; Willis, A. C. J. *Chem. Soc., Dalton Trans.* **1999**, 3451.

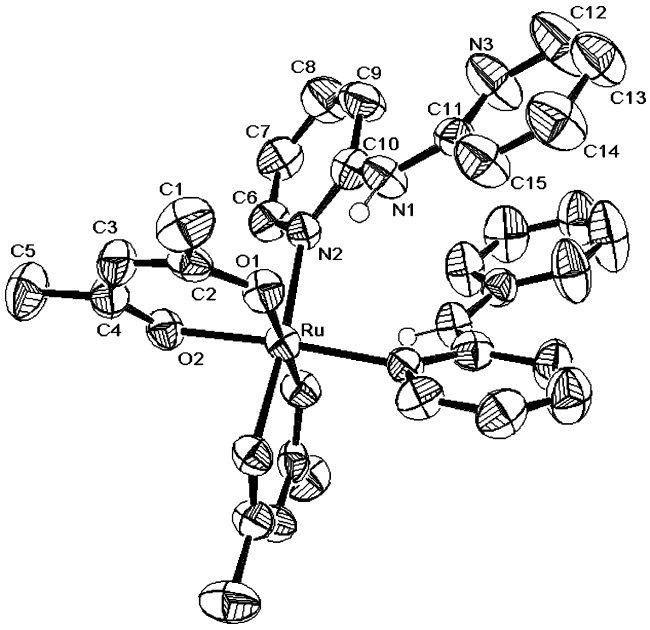

Figure 2. ORTEP diagram of **3**. Hydrogen atoms, with the exception of the N-bonded one, have been omitted for clarity. Ellipsoids are drawn at 50% probability.

in the *trans*- and *cis*-configurations, respectively. The interplanar angles of the two pyridyl rings in the coordinated L are 25.5(0.3)°, 6.1(0.2)°, 22.4(0.2)°, and 18.8(0.3)° for [**1**]ClO_4, **2**, [**2**]ClO_4, and **3**, respectively.[1a,g,6] The greater degree of nonplanarity of monodentate L in **3** as compared to the *trans*-isomer **2** implies the involved steric constrains in the *cis*-orientation of two L in **3**. In moving from **2** to [**2**]ClO_4, molecules reorganize in the lattice to accommodate the perchlorate anions inside the cavity formed down the *c*-axis (Figure S3). The *cis* angle involving the two monodentate dipyridylamine ligands, N(2)−Ru−N(2)#1, in **3** is 97.4(2)°. In **2** and [**2**]ClO_4, the *cis* angles between the interchelate donor centers are O(2)−Ru−O(1)#1, 86.96(7)°, and O(1)−Ru−O(2), 82.25(11)°, respectively. The low symmetry of [**1**]ClO_4 is reflected in its unequal Ru−O [1.999(4)−2.015(5) Å] and Ru−N [2.056(6) and 2.077(6) Å] bond distances.[7a] The Ru−O and Ru−N bond distances in [**1**]ClO_4 are in agreement with the distances reported in $Ru(acac)_3$[7a] and $[Ru(L)_2Cl_2]Cl$, respectively.[7b] The Ru−N bond distance of 2.095(4) Å in **3** is reasonably shorter than that in **2**, 2.1160(19) Å. The relatively stronger $d\pi(Ru^{II}) \rightarrow \pi^*$(L) back-bonding in the *cis*-isomer might be responsible for the shorter Ru−N bond distance in **3** as compared to the *trans*-isomer **2** (see later).[8]

On moving from **2** to [**2**]ClO_4, the Ru−N distance expectedly decreases slightly to 2.105(3) Å. In the structure of **3**, intramolecular hydrogen bonding, O(1)---H−N(1), is present (Figure S4, Table S1).

The ^{1}H NMR spectra of **2** and **3** in $CDCl_3$ are shown in Figure 3. **2** displayed eight partially overlapping but distinct aromatic signals under anaerobic conditions, four doublets and four triplets (δ, 6.3−8.5 ppm, see the Experimental Section) in addition to one NH proton signal at 9.95 ppm as expected from the considerations of half-symmetry and magnetically nonequivalent nature of the two pyridyl rings of L in **2** (Figure 3a). CH and CH_3 protons of acac appeared at 4.94 and 1.63/1.25 ppm, respectively. The ^{1}H NMR spectrum of **2** was also checked up to 243 K; however, the spectral profile and the peak position remained unchanged over the temperature range. The proton resonances of coordinated and uncoordinated pyridine rings of L in **3** overlap and are slightly broadened (δ, 6.85−8.26 ppm, see the Experimental Section), but they do not change over the temperature range of 298−243 K (Figure 3b−d). However, the broad resonance of the amine proton of coordinated L shifts as a function of temperature [δ/ppm, 7.45 (298 K), 7.74 (273 K), 8.19 (243 K)]. It is likely that, in solution, the amine proton fluxionally hydrogen bonds to the uncoordinated pyridine ring of the second L, as well as to the acac ligand as indicated by the crystal structure (Figure S4).

The electrochemically generated **1** and isolated **2** and **3** exhibited one quasi-reversible Ru(III)/Ru(II) couple each in acetonitrile at E_{298}°, $V(\Delta E_p$, mV) of −0.29(85), −0.15(90), and 0.66(90) versus SCE, respectively (Figure S5). Thus, the stability of the Ru(II) state follows the order **3** ≫ **2** > **1**. The presence of two monodentate L's in **2** as compared to one bidentate L in **1** introduces additional stability of the Ru(II) state in **2**. On the other hand, the Ru(III)/Ru(II) potential substantially enhances on switching from *trans*-isomer **2** to *cis*-isomer **3**. For low-spin MA_4B_2 systems where B is a relatively stronger π-acceptor in nature, the redox couple involving d^5−d^6 ions is expected to exhibit $E°(cis) > E°(trans)$ due to better stabilization of the redox orbital in the reduced (d^6) *cis*-isomer.[9] Therefore, in corroboration with the earlier observations,[8] it may be logically stated that the Ru(II) state in **3** is stabilized via the back-bonding. Moreover, the presence of intramolecular hydrogen bonding in **3** (Figure S4) may also be considered as an added factor toward its stabilization in the isolated Ru(II) state. Therefore, despite the quasi-reversible nature of the Ru(III)/Ru(II) couple of **3** on the cyclic voltammetric time scale, the electrochemically generated oxidized species $[\mathbf{3}]^+$ was found to be unstable at 298 K. However, the oxidized *trans*-isomer $[\mathbf{2}]^+$ is stable both in the solid and in the solution states. Poor π-donation being characteristic of Ru(III), back-bonding may be expected to be very weak or totally absent in the trivalent *cis*-isomer $[\mathbf{3}]^+$. Therefore, in the absence of any electronic advantages

(6) Chanda, N.; Mobin, S. M.; Puranik, V. G.; Datta, A.; Niemeyer, M.; Lahiri, G. K. *Inorg. Chem.* **2004**, *43*, 1056.
(7) (a) Chao, G. K. J.; Sime, R. L.; Sime, R. J. *Acta Crystallogr.* **1973**, *B29*, 2845. (b) Berry, J. F.; Cotton, F. A.; Murillo, C. A. *Inorg. Chim. Acta* **2004**, *357*, 3847.
(8) (a) Pramanik, A.; Bag, N.; Ray, D.; Lahiri, G. K.; Chakravorty, A. *Inorg. Chem.* **1991**, *30*, 410. (b) Pramanik, A.; Bag, N.; Ray, D.; Lahiri, G. K.; Chakravorty, A. *J. Chem. Soc., Chem. Commun.* **1991**, 139. (c) Pramanik, A.; Bag, N.; Lahiri, G. K.; Chakravorty, A. *J. Chem. Soc., Dalton Trans.* **1992**, 101. (d) Pramanik, A.; Bag, N.; Lahiri, G. K.; Chakravorty, A. *J. Chem. Soc., Dalton Trans.* **1990**, 3823. (e) Bag, N.; Lahiri, G. K.; Chakravorty, A. *J. Chem. Soc., Dalton Trans.* **1990**, 1557.
(9) Bursten, B. E. *J. Am. Chem. Soc.* **1982**, *104*, 1299.
(10) (a) Richardson, D. E.; Walker, D. D.; Sutton, J. E.; Hodgson, K. O.; Taube, H. *Inorg. Chem.* **1979**, *18*, 2216. (b) Gress, M. E.; Creutz, C.; Quicksall, C. O. *Inorg. Chem.* **1981**, *20*, 1522. (c) Eggleston, D. S.; Goldsby, K. A.; Hodgson, D. J.; Meyer, T. J. *Inorg. Chem.* **1985**, *24*, 4573. (d) Wishart, J. F.; Bino, A.; Taube, H. *Inorg. Chem.* **1986**, *25*, 3318.
(11) (a) Taube, H. *Pure Appl. Chem.* **1979**, *51*, 901. (b) Sekine, M.; Harman, W. D.; Taube, H. *Inorg. Chem.* **1988**, *27*, 3604.

Table 1. Selected Bond Distances (Å) and Angles (deg) for [**1**]ClO_4, **2**, [**2**]ClO_4, and **3**

	[**1**]ClO_4	2	[**2**]ClO_4	3
		Bond Lengths		
Ru−O(1)	1.999(4)	2.0500(15)	1.993(3)	2.042(3)
Ru−O(2)	2.015(5)	2.0474(16)	1.993(3)	2.040(4)
Ru−O(3)	1.994(5)			
Ru−O(4)	2.008(4)			
Ru−N(2)	2.056(6)	2.1160(19)	2.105(3)	2.095(4)
Ru−N(3)	2.077(6)			
N(1)−C(16)	1.373(9)			
N(1)−C(11)	1.372(9)	1.387(3)	1.405(5)	1.401(6)
N(1)−C(10)		1.379(3)	1.350(5)	1.386(6)
		Bond Angles		
O(3)−Ru−O(1)	87.35(19)			
O(3)−Ru−O(4)	91.3(2)			
O(1)−Ru−O(4)	178.6(2)			
O(3)−Ru−O(2)	86.9(2)			
O(1)−Ru−O(2)	93.2(2)	93.04(7)	89.25(11)	93.44(15)
O(4)−Ru−O(2)	86.5(2)			
O(3)−Ru−N(2)	176.5(2)			
O(1)−Ru−N(2)	89.6(2)	88.24(7)	91.63(12)	93.44(16)
O(4)−Ru−N(2)	91.8(2)			
O(2)−Ru−N(2)	91.7(2)	93.24(7)	92.24(11)	87.08(14)
O(3)−Ru−N(3)	93.2(2)			
O(1)−Ru−N(3)	87.7(2)			
O(4)−Ru−N(3)	92.5(2)			
O(2)−Ru−N(3)	179.0(2)			
N(2)−Ru−N(3)	88.4(2)			
O(2)#1−Ru−O(2)		180.0	180.0	88.5(2)
O(2)−Ru−O(1)#1		86.96(7)	90.75(11)	86.47(14)
O(1)#1−Ru−O(1)		180.0	180.0	179.87(19)
O(2)−Ru−N(2)#1		86.76(7)	87.76(11)	175.53(16)
O(1)−Ru−N(2)#1		91.76(7)	88.37(12)	86.64(16)
N(2)#1−Ru−N(2)		180.0	180.0	97.4(2)

Table 2. Crystallographic Data for [**1**]ClO_4, **2**, [**2**]ClO_4, and **3**

	[**1**]ClO_4	2	[**2**]ClO_4	3
molecular formula	$C_{20}H_{23}ClN_3O_8Ru$	$C_{30}H_{32}N_6O_4Ru$	$C_{30}H_{32}ClN_6O_8Ru$	$C_{30}H_{32}N_6O_4Ru$
formula weight	569.93	641.69	741.14	641.69
radiation	Mo Kα	Mo Kα	Mo Kα	Mo Kα
crystal symmetry	monoclinic	monoclinic	monoclinic	orthorhombic
space group	*P*2(1)/*c*	*P*21/*c*	*C*2/*c*	Pcnn
a (Å)	11.730(2)	8.6960(8)	26.6680(17)	11.2430(15)
b (Å)	11.667(2)	9.3830(7)	7.773(3)	12.0250(18)
c (Å)	17.483(4)	18.6479(9)	19.494(4)	21.839(2)
α (deg)	90	90	90.000(17)	90
β (deg)	92.37(3)	107.954(5)	127.129(19)	90
γ (deg)	90	90	90.000(19)	90
V (Å^3)	2390.6(8)	1447.47(19)	3221.7(14)	2952.6(7)
Z	4	2	4	4
μ (mm^{-1})	0.817	0.588	0.628	0.576
T (K)	173(2)	293(2)	293(2)	293(2)
D_{calcd} (g cm^{-3})	1.584	1.472	1.528	1.444
2*θ* range (deg)	3.48−50	4.58−49.86	3.82−49.84	3.72−54.82
e data (R_{int})	4192(0.0407)	2331(0.0000)	2605(0.0226)	3395(0.0000)
R1 ($I > 2\sigma(I)$)	0.0632	0.0246	0.0361	0.0539
wR2 (all data)	0.1368	0.0640	0.0942	0.1162
GOF	1.136	1.089	1.036	0.992

in the trivalent complexes ([**2**]$^+$ and [**3**]$^+$), dipyridylamine−dipyridylamine steric interaction [*cis* [**3**]$^+$ ≫ *trans* [**2**]$^+$] is becoming prominent which eventually destabilizes [**3**]$^+$.[10,11]

The quasi-reversible and irreversible Ru(III)−Ru(IV) processes for **1** and **2** appeared at $E_{298}°$, $V(\Delta E_p$, mV) of 1.27 (90) and E_{pa} of 1.5 V, respectively.

Electronic spectra of the complexes in CH_3CN are shown in Figure S6, and the data are shown in the Experimental Section. The ligand-based multiple strong transitions appeared in the UV region for all of the complexes. The lowest energy MLCT transitions, presumably due to Ru(II) → L, appeared at 526, 492, and 671 nm for **1**, **2**, and **3**, respectively, with a substantial difference in intensity.[6,12] Thus, a wide variation in energy (492−671 nm) and intensity has been observed depending on the binding mode of L and the specific geometrical configuration. The trivalent congeners [**1**]$^+$ and [**2**]$^+$ exhibited broad LMCT transitions at 542

(12) (a) Patra, S.; Sarkar, B.; Ghumaan, S.; Fiedler, J.; Zalis, S.; Kaim, W.; Lahiri, G. K. *Dalton Trans.* **2004**, 750. (b) Patra, S.; Sarkar, B.; Ghumaan, S.; Fiedler, J.; Kaim, W.; Lahiri, G. K. *Dalton Trans.* **2004**, 754. (c) Patra, S.; Sarkar, B.; Mobin, S. M.; Kaim, W.; Lahiri, G. K. *Inorg. Chem.* **2003**, *42*, 6469. (d) Patra, S.; Miller, T. A.; Sarkar, B.; Niemeyer, M.; Ward, M. D.; Lahiri, G. K. *Inorg. Chem.* **2003**, *42*, 4707. (e) Patra, S.; Mondal, B.; Sarkar, B.; Niemeyer, M.; Lahiri, G. K. *Inorg. Chem.* **2003**, *42*, 1322.

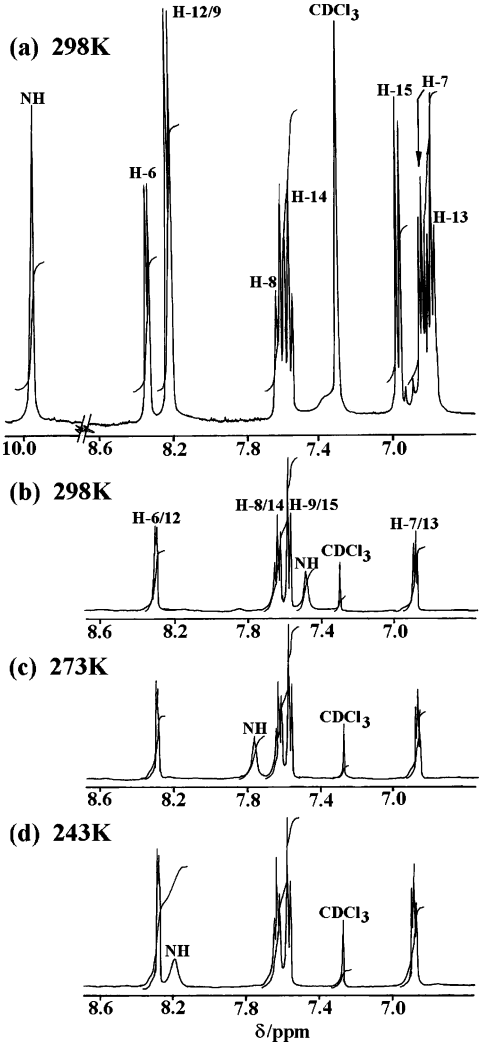

Figure 3. ^{1}H NMR spectra (aromatic region) in $CDCl_3$ of (a) *trans*-Ru(acac)$_2$(L)$_2$ (**2**) at 298 K, (b) *cis*-Ru(acac)$_2$(L)$_2$ (**3**) at 298 K, (c) *cis*-Ru(acac)$_2$(L)$_2$ (**3**) at 273 K, and (d) *cis*-Ru(acac)$_2$(L)$_2$ (**3**) at 243 K.

and 574 nm, respectively, in addition to the intraligand transitions in the UV-region.

The trivalent complex $[\mathbf{1}]^+$ exhibited magnetic moment of 1.84 μ_B at 298 K in the solid state corresponding to one-unpaired electron as expected from the low-spin Ru(III) octahedral species.[13] Consequently, $[\mathbf{1}]^+$ exhibited a rhombic EPR spectrum in chloroform glass at 77 K ($g_1 = 2.484$, $g_2 = 2.133$, $g_3 = 1.637$, Figure S7).[14] The g anisotropy $g_1 - g_3 = 0.496$, and the average g factor of $\langle g \rangle = 2.113$, derived from $\langle g \rangle = [1/3(g_1^2 + g_2^2 + g_3^2)]^{1/2}$,[15] implies a slightly distorted octahedral arrangement around the ruthenium ion as observed from its molecular structure in the solid state. Similarly, $[\mathbf{1}]ClO_4$ in the solid state displayed a poorly resolved rhombic EPR spectrum at 77 K ($g_1 = 2.402$, $g_2 = 2.133$, $g_3 = 1.801$, Figure S7, inset) with an average g factor of $\langle g \rangle = 2.126$. However, no EPR signal was observed at room temperature both in the solid state and in the fluid medium, which signifies rapid relaxation due to paramagnetic states lying close to the doublet ground state.

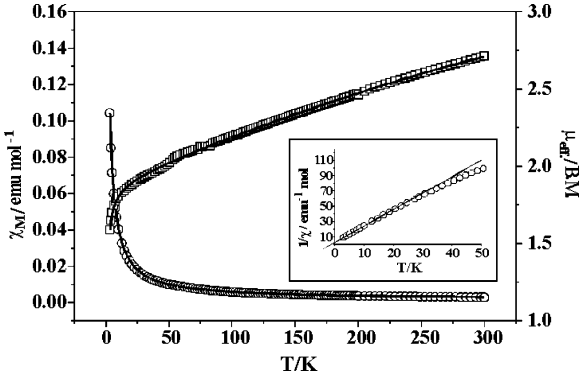

Figure 4. Temperature dependence of the magnetic susceptibility (○) and magnetic moment (□) for complex $[\mathbf{2}]ClO_4$. Solid lines result from least-squares fits using eq 2. Inset shows the fit of $1/\chi$ in the temperature range of 3−25 K.

In contrast to the magnetic moment obtained for complex $[\mathbf{1}]ClO_4$ (1.84 μ_B at 298 K), $[\mathbf{2}]ClO_4$ exhibited a magnetic moment of 2.71 μ_B at 300 K in the solid state, higher than that expected for a low-spin Ru(III) complex. The variable-temperature magnetic measurements showed a pronounced decrease of the magnetic moment with temperature, that dropped to 1.59 μ_B at 3 K.

The unusual high value of the magnetic moment at room temperature for $[\mathbf{2}]ClO_4$ could be due to the presence of an important nonquenched spin−orbit coupling. The magnetic susceptibility for a low-spin d^5 ion, with spin−orbit coupling, can be expressed[16] by eq 1:

$$\chi_M = \frac{Ng^2\beta^2}{3kT}\frac{8 + \left(\frac{3\lambda}{kT} - 8\right)\exp\left(-\frac{3\lambda}{2kT}\right)}{4\frac{\lambda}{kT}\left(2 + \exp\left(-\frac{3\lambda}{2kT}\right)\right)} \qquad (1)$$

The experimental magnetic data for complex $[\mathbf{2}]ClO_4$ cannot be fitted using this equation. However, when a term corresponding to the temperature-independent paramagnetism (TIP) is included, the magnetic data fit well in the temperature range 50−300 K, but it fails from 50 to 3 K. The pronounced decreases of the magnetic moment at very low temperature indicate some degree of antiferromagnetic coupling. In fact, the magnetic susceptibility below 25 K obeys the Curie−Weiss law with $\theta = -1.50$ K. Using the expression $\theta = 2JS(S+1)/3k$, an antiferromagnetic coupling (J) of -2.07 cm^{-1} is calculated (Figure 4, inset). The existence of weak but nonnegligible antiferromagnetic coupling at very low temperature in molecular complexes is not unusual in ruthenium chemistry.[17]

(13) (a) Munshi, P.; Samanta, R.; Lahiri, G. K. *J. Organomet. Chem.* **1999**, *586*, 176. (b) Ghosh, P.; Pramanik, A.; Bag, N.; Lahiri, G. K.; Chakravorty, A. *J. Organomet. Chem.* **1993**, *454*, 237. (c) Bag, N.; Lahiri, G. K.; Bhattacharya, S.; Falvello, L. R.; Chakravorty, A. *Inorg. Chem.* **1988**, *27*, 4396. (d) Ramanathan, H.; Santra, B. K.; Lahiri, G. K. *J. Organomet. Chem.* **1997**, *540*, 155.

(14) (a) Chanda, N.; Sarkar, B.; Fiedler, J.; Kaim, W.; Lahiri, G. K. *Dalton Trans.* **2003**, 3550. (b) Poppe, J.; Moscherosch, M.; Kaim, W. *Inorg. Chem.* **1993**, *32*, 2640.

(15) Kaim, W. *Coord. Chem. Rev.* **1987**, *76*, 187.

(16) Mabs, F. E.; Machin, D. J. *Magnetism and Transition Metal Complexes*; Chapman and Hall Ltd.: London, 1973.

(17) (a) Barral, M. C.; Jiménez-Aparicio, R.; Pérez-Quintanilla, D.; Priego, J. L.; Royer, E. C.; Torres, M. R.; Urbanos, F. A. *Inorg. Chem.* **2000**, *39*, 65. (b) Barral, M. C.; González-Prieto, R.; Jiménez-Aparicio, R.; Priego, J. L.; Torres, M. R.; Urbanos, F. A. *Eur. J. Inorg. Chem.* **2003**, 2339.

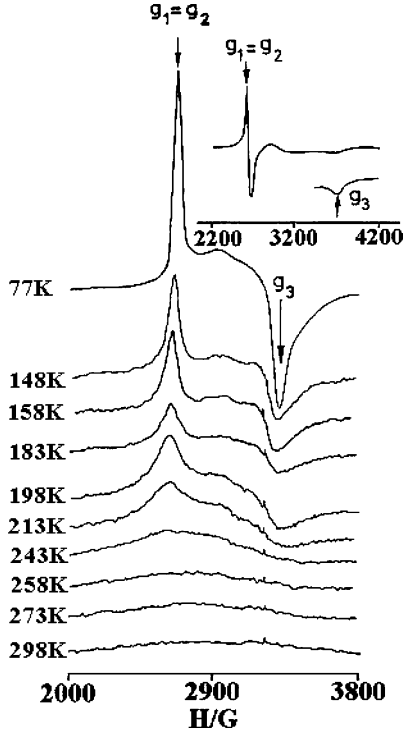

Figure 5. Variable-temperature EPR spectra of [**2**]ClO_4 in the solid state. The inset shows the EPR spectrum of [**2**]ClO_4 in $CHCl_3$ at 77 K.

The complete experimental data can be satisfactorily fitted (Figure 4) using eq 2 that considers a Weiss constant in addition to the temperature-independent paramagnetism:

$$\chi_M = \frac{Ng^2\beta^2}{3k(T-\theta)} \frac{8 + \left(\frac{3\lambda}{kT} - 8\right)\exp\left(-\frac{3\lambda}{2kT}\right)}{4\frac{\lambda}{kT}\left(2 + \exp\left(-\frac{3\lambda}{2kT}\right)\right)} + \text{TIP} \quad (2)$$

The parameters obtained from this fit, together with σ^2 indicate the quality of the fit, have been collected in Table 3. The g value (2.16) is close to that obtained from the EPR spectrum (2.286, see below). The θ and J values are slightly higher than those calculated for other mononuclear Ru(III) complexes[18] as $CsRu(SO_4)_2 \cdot 12H_2O$ and $Ru(acac)_3$, but the difference is in accordance with the pronounced decrease of the magnetic moment at low temperature observed in complex [**2**]ClO_4. On the other hand, the θ and J values of -1.26 K and -1.73 cm^{-1}, respectively, are also consistent with the values obtained in the fit of $1/\chi$ from 3 to 25 K. The J value confirms the existence of a weak antiferromagnetic coupling in the complex. The calculated spin−orbit coupling constant of -690 cm^{-1} is consistent with a Ru(III) complex.[19] The TIP value of 5×10^{-4} cm^3/mol is also usual in ruthenium complexes.[19b]

The variable-temperature EPR spectra of [**2**]ClO_4 in the solid state are shown in Figure 5. It failed to show any signal up to 243 K. However, the signals started developing from 213 K and the intensity kept on increasing with further lowering in temperature. At 77 K, a well-resolved axial spectrum ($g_1 = g_2 = 2.428$ and $g_3 = 1.972$; $\langle g \rangle = 2.286$) was observed as expected from the *trans* orientation of the two monodentate L's in the low-spin $[Ru^{III}(acac)_2(L)_2]^+$.[8d] The observed axial EPR spectrum of [**2**]ClO_4 at 77 K finds justification from its solid-state magnetic moment of 1.92 μ_B at 77 K (obtained from the variable-temperature magnetic moment measurements, Figure 4) corresponding to one unpaired electron. The $CHCl_3$ solution of $[\mathbf{2}]^+$ also failed to show any EPR signal at room temperature; however, it exhibited a clear axial spectrum ($g_1 = g_2 = 2.452$ and $g_3 = 1.750$; $\langle g \rangle = 2.243$) at 77 K (Figure 5, inset).

Table 3. Calculated Magnetic Parameters for [**2**]ClO_4[a,b]

g	2.16
λ (cm^{-1})	−690
θ (K)	−1.26 (−1.50)
J (cm^{-1})	−1.73 (−2.07)
TIP (cm^3/mol)	5×10^{-4}
σ^2	1.2×10^{-5}
$\sigma^2 = \sum(\mu_{\text{eff.calc.}} - \mu_{\text{eff.exp.}})^2/\sum\mu_{\text{eff.exp.}}{}^2$	

[a] Using eq 2 in the text. [b] The θ and J values calculated using the Curie−Weiss law in the temperature range 3−25 K are given in parentheses.

Conclusion

The present article demonstrates the following important features: (i) the unique metal−ligand combination of $\{Ru(acac)_2\}$ and 2,2′-dipyridylamine (L) stabilizes the unusual monodentate binding mode of L in the isomeric complexes, *trans*-$[(acac)_2Ru^{II}(L)_2]$ (**2**), *trans*-$[(acac)_2Ru^{III}(L)_2]$-ClO_4 ([**2**]ClO_4), and *cis*-$[(acac)_2\,Ru^{II}\,(L)_2]$ (**3**); (ii) preferential stabilization of two sterically constrained monodentate L's in the *cis* configuration (motif **E**) particularly in an environment where the usual bidentate mode of L (motif **A**) in $[(acac)_2Ru^{III}L]ClO_4$ ([**1**]ClO_4) is also found to be equally stable; (iii) the stability of the Ru(II) state follows the order **1** < **2** ≪ **3**, where relatively stronger π-back-bonding in the *cis* geometry destabilizes the Ru(III) state in **3** substantially; and (iv) the anomalous magnetic moment of the trivalent ruthenium(III) complex, [**2**]ClO_4 (2.71 μ_B at 300 K which drops to 1.59 μ_B at 3 K), has been interpreted via eq 2 which considers nonquenched spin−orbit coupling and Weiss constant in addition to the temperature-independent paramagnetism.

Experimental Section

The starting complex *cis*-$[Ru(acac)_2(CH_3CN)_2]$ was prepared according to the reported procedure.[20] 2,2′-Dipyridylamine (L) was purchased from Aldrich. Other chemicals and solvents were reagent grade and used as received. For spectroscopic and electrochemical studies, HPLC-grade solvents were used. Solution electrical conductivity was checked using a Systronic conductivity bridge 305. Infrared spectra were taken on a Nicolet spectrophotometer with samples prepared as KBr pellets. The ^1H NMR spectra of **2** and **3** were obtained on 300-MHz Varian and 500-MHz Bruker FT-NMR spectrometers, respectively. UV−vis spectral studies were performed on a Jasco-570 spectrophotometer. Cyclic voltammetric and coulometric measurements were carried out using a PAR model 273A electrochemistry system. A platinum wire working electrode,

(18) (a) Bernhard, P.; Stebler, A.; Ludi, A. *Inorg. Chem.* **1984**, *23*, 2151. (b) Figgis, B. N.; Reynolds, P. A.; Murray, K. S. *Aust. J. Chem.* **1998**, *51*, 229.

(19) (a) Carlin, R. L. *Magnetochemistry*; Springer- Verlag: Berlin, 1986. (b) Bendix, J.; Steenberg, P.; Sotofte, I. *Inorg. Chem.* **2003**, *42*, 4510.

(20) Kobayashi, T.; Nishina, Y.; Shimizu, K. G.; Sato, G. P. *Chem. Lett.* **1988**, 1137.

a platinum wire auxiliary electrode, and a saturated calomel reference electrode (SCE) were used in a standard three-electrode configuration. Commercial tetraethylammonium bromide was converted to pure tetraethylammonium perchlorate (TEAP) by following an available procedure.[21] TEAP was the supporting electrolyte, and the solution concentration was ca. 10^{-3} M; the scan rate used was 50 mV s^{-1}. The half wave potential $E_{298}°$ was set equal to $0.5(E_{pa} + E_{pc})$, where E_{pa} and E_{pc} are anodic and cathodic cyclic voltammetric peak potentials, respectively. A platinum gauze working electrode was used in the coulometric experiments. All electrochemical experiments were carried out under dinitrogen atmosphere. The variable-temperature magnetic susceptibility data were measured on a Quantum Design MPMS*XL* SQUID (Superconducting Quantum Interference Device) susceptometer over a temperature range of 3−300 K. Each raw data field was corrected for the diamagnetic contribution of both the sample holder and the compound to the susceptibility. The molar diamagnetic corrections for the complexes were calculated on the basis of Pascal's constants. The fit of experimental data was carried out using the commercial MATLAB V.5.1.0.421 program, fitting all parameters simultaneously. The EPR measurements were made with a Varian model 109C E-line X-band spectrometer fitted with a quartz dewar. The elemental analyses were carried out with a Perkin-Elmer 240C elemental analyzer. Electrospray mass spectra were recorded on a Micromass Q-ToF mass spectrometer.

Synthesis of [1]ClO_4, 2, [2]ClO_4, and 3. 2,2′-Dipyridylamine (90 mg, 0.52 mmol) was added to the starting complex *cis*-$Ru(acac)_2(CH_3CN)_2$ (100 mg, 0.26 mmol) in ethanol (20 mL). The resulting mixture was heated to reflux under aerobic conditions for 12 h. The solvent was then removed under reduced pressure. The solid mass thus obtained was purified via a silica gel column. Initially, the neutral complexes **2** (yellow) and **3** (green) were eluted by 10:1 CH_2Cl_2−CH_3CN and 5:1 CH_2Cl_2−CH_3CN, respectively. The trivalent complexes [**2**]ClO_4 (blue) and [**1**]ClO_4 (purple) were eluted later on by using excess $NaClO_4$ (40 mg, 3.3 mmol) solution in 100 mL of 1:1 CH_2Cl_2−CH_3CN and CH_3CN, respectively. The crystalline solid complexes were obtained via the removal of solvent under reduced pressure. **2** and **3** were then recrystallized from 1:1 dichloromethane−hexane, and [**1**]ClO_4 and [**2**]ClO_4 were recrystallized from 1:1 acetonitrile−benzene.

Complex 2. Yield: 12% (20 mg). Anal. Calcd for $C_{30}H_{32}O_4N_6Ru$ (**2**): C, 56.15; H, 5.03; N, 13.10. Found: C, 55.83; H, 5.46; N, 12.85. λ_{max}/nm (ϵ/M^{-1} cm^{-1}) in acetonitrile: 492(4229), 444(4695), 312(24 414), 264(39 958), 198(45 176). ν_{NH}: 3282 cm^{-1}. The electrospray mass spectrum in acetonitrile [Supporting Information (Figure S8)] showed the peaks centered at m/z = 642.07 and 471 corresponding to $[\mathbf{2}]^+$ (calculated molecular mass: 641.69) and $[\mathbf{2} - \mathbf{L}]^+$ (calculated molecular mass: 470.5), respectively. ^{1}H NMR [δ/ppm (J/H_z)]: H6 [8.36(5.4)], H12/H9 [8.25(7.5)], H8 [7.58-(8.4,9.2)], H14 [7.52(9.2,7.2)], H15 [6.96(8.1)], H7 [6.78(5.1,6.9)], H13 [6.72(6.3,6.6)], CH (4.96), NH (9.95), CH_3 (1.63 and 1.25).

Complex 3. Yield: 16% (27 mg). Anal. Calcd for $C_{30}H_{32}O_4N_6$-Ru (**3**): C, 56.15; H, 5.03; N, 13.10. Found: C, 56.53; H, 4.86; N, 12.88. λ_{max}/nm (ϵ/M^{-1} cm^{-1}) in acetonitrile: 671(1086), 432(2544), 352(10 561), 308(23 200), 268(34 900). ν_{NH}: 3280 cm^{-1}. The electrospray mass spectrum in acetonitrile [Supporting Information (Figure S9)] showed the peaks centered at m/z = 642.08 and 471.02 corresponding to $[\mathbf{3}]^+$ (calculated molecular mass: 641.69) and $[\mathbf{3} - \mathbf{L}]^+$ (calculated molecular mass: 470.5), respectively. ^{1}H NMR [δ/ppm (J/H_z)]: H6/H12 [8.26(5.0)], H8/H14 [7.60(8.0,7.5)], H9/H15 [7.54(8.0)], H7/H13 [6.85(5.5,6.5)], CH (5.28), NH (7.45), CH_3 (1.71 and 1.26).

Complex [2]ClO_4. Yield: 18% (35 mg). Anal. Calcd for $C_{30}H_{32}O_8N_6RuCl$ ([**2**]ClO_4): C, 48.62; H, 4.35; N, 11.34. Found: C, 48.73; H, 3.99; N, 11.65. Molar conductivity [Λ_M/Ω^{-1} cm^2 M^{-1}] in acetonitrile: 115. λ_{max}/nm (ϵ/M^{-1} cm^{-1}) in acetonitrile: 574(2964), 324(24 193), 290(25 236), 262(37 158), 198(47 916). $\nu(ClO_4^-)$: 1097 and 624 cm^{-1}. and ν_{NH}: 3300 cm^{-1}. Crystal structure of [**2**]-ClO_4 is shown in Figure S2. The electrospray mass spectrum in acetonitrile [Supporting Information (Figure S10)] showed the peaks centered at m/z = 642.13 and 471.05 corresponding to $[[\mathbf{2}]ClO_4 - ClO_4]^+$ (calculated molecular mass: 641.69) and $[[\mathbf{2}]ClO_4 - L - ClO_4]^+$ (calculated molecular mass: 470.5), respectively.

Complex [1]ClO_4. Yield: 27% (40 mg). Anal. Calcd for $C_{20}H_{23}O_8RuN_3Cl$ ([**1**]ClO_4): C, 42.15; H, 4.07; N, 7.37. Found: C, 42.43; H, 4.36; N, 7.65. Molar conductivity [Λ_M(Ω^{-1} cm^2 M^{-1})] in acetonitrile: 125. λ_{max}/nm (ϵ/M^{-1} cm^{-1}) in acetonitrile: 542(1884), 324(11 000), 270(24 234), 240(16 523), 212(15 366). $\nu(ClO_4^-)$: 1112 and 624 cm^{-1}. ν_{NH}: 3302.4 cm^{-1}. Crystal structure of [**1**]ClO_4 is shown in Figure S2. The electrospray mass spectrum in acetonitrile [Supporting Information (Figure S11)] showed the molecular ion peak centered at m/z = 471.06 corresponding to $[([\mathbf{1}]ClO_4) - ClO_4]^+$ (calculated molecular mass: 470.5).

Crystal Structure Determination. Single crystals were grown by slow diffusion of hexane into dichloromethane solution of [**1**]ClO_4 or **2** or **3**, followed by slow evaporation. Single crystals of [**2**]ClO_4 were grown by slow diffusion of benzene into an acetonitrile solution of the compound followed by slow evaporation. The data for [**1**]ClO_4 were collected at 173 K using a Siemens P3 diffractometer. The data for **2**, [**2**]ClO_4, and **3** were collected at 293 K on a Enraf-Nonius CAD4 (MACH-3) diffractometer. Selected data collection parameters and other crystallographic data are summarized in Table 2. Calculations for [**1**]ClO_4, **2**, [**2**]ClO_4, and **3** were carried out with the SHELXTL PC 5.03[22]/SHELXL-97[23] and SHELXS-97/SHELXL-97[23] program systems installed on local personal computers. The phase problem was solved by direct methods, and the structure was refined on F_o^2 by full-matrix least-squares refinement. An absorption correction was applied by using semiempirical ψ-scans. Anisotropic thermal parameters were refined for all non-hydrogen atoms. The Cl−O distances for the perchlorate anion in [**1**]ClO_4 were restrained to be equal. H-atoms were placed in the idealized positions and refined in a riding model approximation with a common isotropic displacement parameter for CH- and CH_3-groups, respectively. The position of the N-bonded H-atom was allowed to refine freely.

Acknowledgment. We thank the Department of Science and Technology and Council of Scientific and Industrial research, New Delhi, India, for financial support. The X-ray structural studies of **2**, [**2**]ClO_4, and **3** were carried out at the National Single Crystal Diffractometer Facility, Indian Institute of Technology, Bombay. Special acknowledgment is made to the Sophisticated Analytical Instrument Facility, Indian Institute of Technology, Bombay, for providing the NMR and EPR facilities. The referees' comments at the revision stage were very helpful.

Supporting Information Available: X-ray crystallographic data for the complexes [**1**]ClO_4, **2**, [**2**]ClO_4, and **3** in CIF format; ORTEP

(21) Sawyer, D. T.; Sobkowiak, A.; Roberts, J. L., Jr. *Electrochemistry for Chemists*; Wiley: New York, 1995.

(22) *SHELXTL PC 5.03*; Siemens Analytical X-ray Instruments Inc.; Madison, WI, 1994.

(23) Sheldrick, G. M. *Program for Crystal Structure Solution and Refinement*; Universität Göttingen, Göttingen, Germany, 1997.

diagrams of [**1**]ClO_4 and [**2**]ClO_4 (Figures S1 and S2); packing diagrams of **2** and [**2**]ClO_4 (Figure S3); intramolecular hydrogen bonding in **3** (Figure S4, Table S1); cyclic voltammograms of **1**, **2**, and **3** (Figure S5); UV−vis spectra of **1**, **2**, **3**, [**1**]ClO_4, and [**2**]ClO_4 (Figure S6); EPR spectra of [**1**]ClO_4 (Figure S7) and electrospray mass spectra of **2**, **3**, [**2**]ClO_4, and [**1**]ClO_4 (Figures S8−S11); and suggested pathway for the simultaneous formations of *trans* (**2**) and *cis* (**3**) species (Scheme S1). This material is available free of charge via the Internet at http://pubs.acs.org.

IC049219V